

CAUGHT IN THE ACT: THE ONSET OF MASSIVE STAR FORMATION

H. BEUTHER,^{1,2} T. K., SRIDHARAN,¹ AND M. SAITO³

Received 2005 August 19; accepted 2005 October 17; published 2005 November 15

ABSTRACT

Combining mid-infrared data from the *Spitzer Space Telescope* with cold gas and dust emission observations from the Plateau de Bure Interferometer, we characterize the infrared dark cloud IRDC 18223–3 at high spatial resolution. The millimeter continuum data reveal a massive $\sim 184 M_{\odot}$ gas core with a projected size of $\sim 28,000$ AU that has no associated protostellar mid-infrared counterpart. However, the detection of $4.5 \mu\text{m}$ emission at the edge of the core indicates early outflow activity, which is supported by broad CO and CS spectral line-wing emission. Moreover, systematically increasing $\text{N}_2\text{H}^+(1-0)$ line width toward the millimeter core center can be interpreted as additional evidence for early star formation. Furthermore, the $\text{N}_2\text{H}^+(1-0)$ line emission reveals a less massive secondary core that could be in an evolutionary stage prior to any star formation activity.

Subject headings: stars: early-type — stars: formation — stars: individual (IRDC 18223–3) — stars: winds, outflows

1. INTRODUCTION

Massive-star-formation research has focused so far either on evolutionary stages observable in the centimeter regime due to free-free emission (ultracompact H II regions; e.g., Kurtz et al. 2000; Churchwell 2002) or slightly younger stages that emit in the (sub)millimeter bands and are also detectable at mid-infrared (MIR) wavelengths due to warm dust emission (e.g., Molinari et al. 1996; Sridharan et al. 2002). The initial phase prior to any cm free-free and MIR warm dust emission was observationally largely inaccessible. The most basic identification criterion for the initial stages of massive star formation is that such regions have to be bright in the (sub)millimeter regime due to cold dust and gas, and weak or undetected in the MIR due to the absence or weakness of warm dust emission. MIR surveys conducted with the *Midcourse Space Experiment (MSX)* and the *Infrared Space Observatory* permitted identification of a large number of infrared dark clouds (IRDCs; e.g., Egan et al. 1998). Studies of low-mass IRDCs have constrained the initial conditions of low-mass star formation quite well (e.g., Andre et al. 2000; Bacmann et al. 2000; Alves et al. 2001; Kirk et al. 2005), but the high-mass regime is just beginning to be explored (e.g., Garay et al. 2004; Hill et al. 2005; Klein et al. 2005; Sridharan et al. 2005).

In a 1.2 mm continuum study of high-mass protostellar objects (HMPOs) associated with *Infrared Astronomical Satellite (IRAS)* sources, we observed serendipitously within the same fields additional millimeter peaks not associated with any *IRAS* source (Beuther et al. 2002a). Correlation of these millimeter peaks with the *MSX* MIR data revealed a sample of millimeter peaks that is not only weak in the MIR but is seen as absorption shadows against the Galactic background (Sridharan et al. 2005). Mass estimates based on the 1.2 mm continuum emission show that they are massive gas cores (of the order a few $100 M_{\odot}$), making them potential high-mass starless core (HMSC) candidates. Figure 1 shows the HMSC candidate region IRDC 18223–3, which is a 1.2 mm continuum peak at

a distance of ~ 3.7 kpc (Sridharan et al. 2005) in a dust and gas filament approximately $3'$ south of IRAS 18223–1243 (peak 3 in Beuther et al. 2002a). While the MIR absorption puts the source in the sample of potential HMSCs, a NH_3 rotation temperature of ~ 33 K indicates probable early star formation activity (Sridharan et al. 2005). The region was also identified recently as a massive dense core by Garay et al. (2004).

2. OBSERVATIONS

We observed IRDC 18223–3 with the Plateau de Bure Interferometer (PdBI) during three nights in 2004/2005 at 93 GHz in the C and D configuration, covering projected baselines between 15 and 230 m. The 3 mm receivers were tuned to the $\text{N}_2\text{H}^+(1-0)$ line at 93.174 GHz. The phase noise was lower than 30° , and atmospheric phase correction based on the 1.3 mm total power was applied. For continuum measurements, we placed two 320 MHz correlator units in the band. The N_2H^+ lines were excluded in averaging the two units to produce the final continuum image. Temporal fluctuations of amplitude and phase were calibrated with frequent observations of the quasars 1741–038 and 1908–201. The amplitude scale was derived from measurements of MWC 349. We estimate the final flux accuracy to be correct to within $\sim 15\%$. The phase reference center is R.A. = $18^{\text{h}}25^{\text{m}}08^{\text{s}}.3$ (J2000.0) and decl. = $-12^{\circ}45'26''.90$ (J2000.0), and the velocity of rest v_{lsr} is 45 km s^{-1} . The synthesized beam of the observations is $5''.8 \times 2''.4$ (P.A. = 14°). The 3σ continuum rms is $1.08 \text{ mJy beam}^{-1}$. These millimeter observations are complemented with MIR *Spitzer* data from the GLIMPSE survey of the Galactic plane using the Infrared Array Camera (IRAC) centered at 3.6, 4.5, 5.8, and $8.0 \mu\text{m}$ (Werner et al. 2004; Fazio et al. 2004; Benjamin et al. 2003). Observational details for the CO (2–1) and CS (2–1) observations were given in Sridharan et al. (2002) and Beuther et al. (2002a).

3. RESULTS AND DISCUSSION

Figure 2 presents the MIR data toward IRDC 18223–3 as a three-color composite overlaid with contours of the 93 GHz millimeter continuum emission. We detect a compact dust and gas core that is spatially coincident with the MIR dark lane, but we do not detect a (proto)stellar MIR counterpart down to the

¹ Harvard-Smithsonian Center for Astrophysics, 60 Garden Street, Cambridge, MA 02138; hbeuther@cfa.harvard.edu, tksridha@cfa.harvard.edu.

² Max-Planck-Institute for Astronomy, Königstuhl 17, 69117 Heidelberg, Germany; beuther@mpia.de.

³ National Astronomical Observatory of Japan, 2-21-1 Osawa, Mitaka, Tokyo 181-8588, Japan; masao.saito@nao.ac.jp.

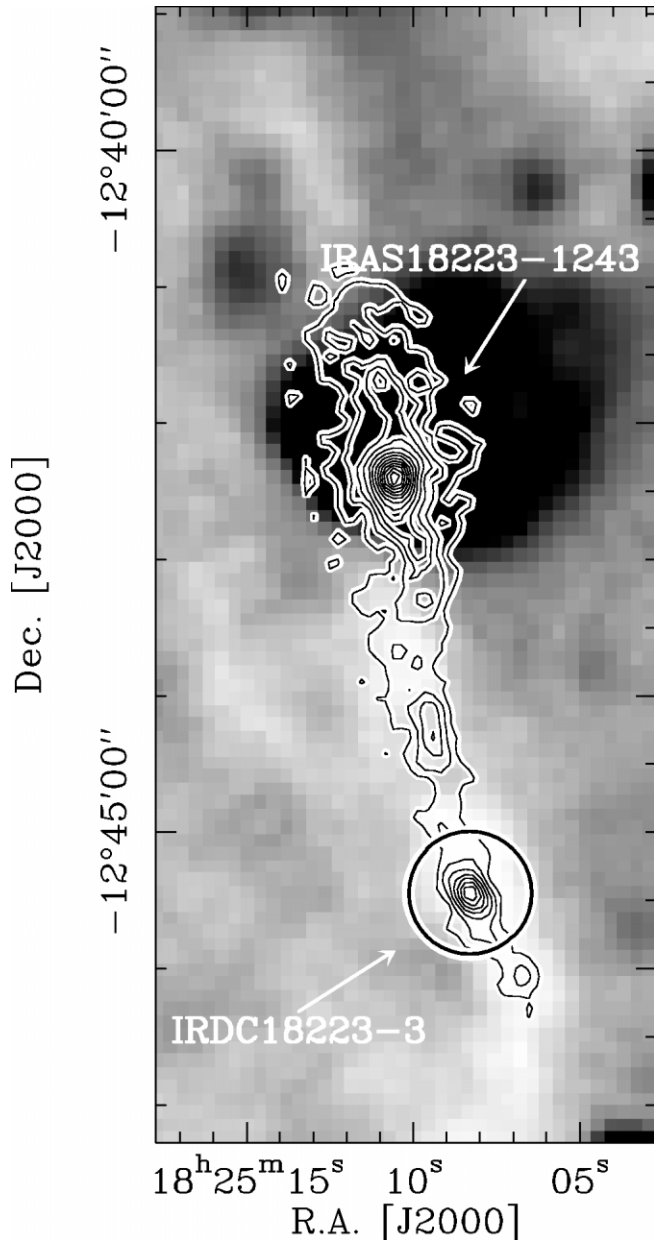


FIG. 1.—Contour overlay of the 1.2 mm single-dish continuum map (Beuther et al. 2002a) on the 8 μm MSX image (gray scale). The contour levels are from 38 mJy in 38 mJy steps. The northern source is the HMPO IRAS 18223–1243, and the southern source is the HMSC candidate IRDC 18223–3. The black circle outlines the primary beam of the PdBI observations.

sensitivity limit of this data (3σ ; 0.05 mJy at 3.6 μm , 0.05 mJy at 4.5 μm , 0.13 mJy at 5.8 μm , and 0.15 mJy at 8.0 μm). The projected size of the millimeter core in the east-west direction is $\sim 28,000$ AU. Assuming the 93 GHz continuum is due to optically thin thermal dust emission, we estimate the mass and column density of the core, following Beuther et al. (2002a). Using the temperature of 33 K from NH_3 observations (Sridharan et al. 2005) and a dust opacity index $\beta = 2$, we calculate the mass within the 50% contour level (integrated flux $S_{50\%} \sim 6.7$ mJy) to be $\sim 95 M_\odot$, and the mass within the 3σ level of 1.08 mJy ($S_{3\sigma} \sim 13.0$ mJy) to be $\sim 184 M_\odot$. The peak flux of ~ 5.1 mJy beam^{-1} converts to a peak column density of $\sim 1.0 \times 10^{24} \text{ cm}^{-2}$, corresponding to a visual extinction of $A_v = N_{\text{H}_2}/0.94 \times 10^{21} \sim 1000$ (Frerking et al. 1982). The uncertainties for mass and column density estimates from dust

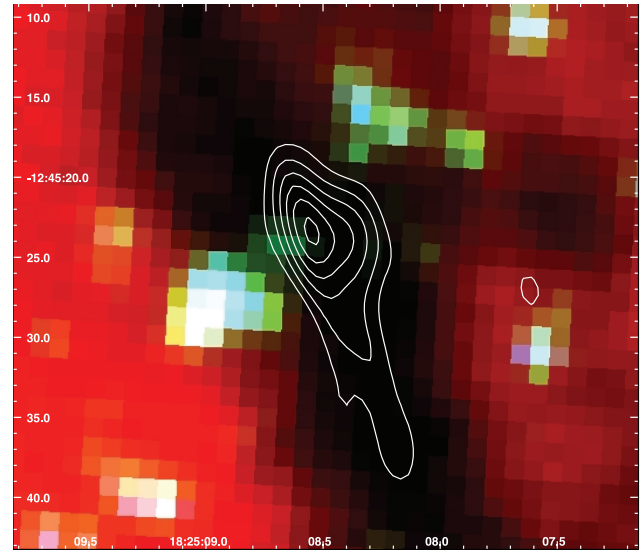


FIG. 2.—Three-color image of the *Spitzer* IRAC observations at 3.6 (blue), 4.5 (green), and 8.0 μm (red). The contours show the PdBI 93 GHz continuum map from 1.08 mJy (3σ) in 0.72 mJy steps (2σ). The axes are in R.A. (J2000.0) and decl. (J2000.0).

continuum emission are approximately within a factor of 5 (e.g., Beuther et al. 2002a). Single-dish 1.2 mm continuum data (Beuther et al. 2002a) result using the same assumptions in a total mass estimate of $\sim 245 M_\odot$, implying $\sim 25\%$ of missing flux in the PdBI data, due to missing short spacings. The data clearly show that we are dealing with a massive gas core at an early evolutionary stage.

While we do not detect a protostellar MIR source toward the millimeter-peak IRDC 18223–3, Figure 2 shows weak emission in the *Spitzer* 4.5 μm band (IRAC band 2, color-coded in green) toward the southeast, the northwest, and at the western edge of the millimeter core. These features are just detected in IRAC band 2. Since a foreground source would also show up at 3.6 μm , and an embedded protostellar object would be red and thus also detectable at 5.8 and 8.0 μm if PAH (polycyclic aromatic hydrocarbon) features are not too bright, these 4.5 μm features are unlikely to be of a (proto)stellar nature. One cannot entirely exclude that the 4.5 μm emission is due to highly reddened background sources (e.g., the MIR lower limit magnitudes imply minimum visual extinctions $A_v > 40$ and $A_v > 120$ for the southeastern and the western 4.5 μm features, respectively), but it is more likely that the 4.5 μm features are due to line emission within the IRAC band 2 bandpass (approximately 4–5 μm). *Spitzer* outflow observations showed that molecular outflows are particularly strong in the 4.5 μm band, because of H_2 and CO line emission (e.g., Noriega-Crespo et al. 2004). Hence, we suggest that the 4.5 μm emission at the edge of the millimeter core may be due to shock excitation as the outflow collides with the ambient molecular medium. The two 4.5 μm features to the southeast and northwest are on opposite sides of the main millimeter peak, which is indicative of typical bipolar outflows (Richer et al. 2000). The additional third feature to the west is suggestive of multiple outflows, as is often observed in massive star-forming regions (e.g., Beuther et al. 2003).

Support for this outflow interpretation is provided by single-dish CO (2–1) and CS (2–1) observations from the Caltech Submillimeter Observatory (CSO) and the IRAM 30 m telescope (Sridharan et al. 2002; Beuther et al. 2002a). Both spectra

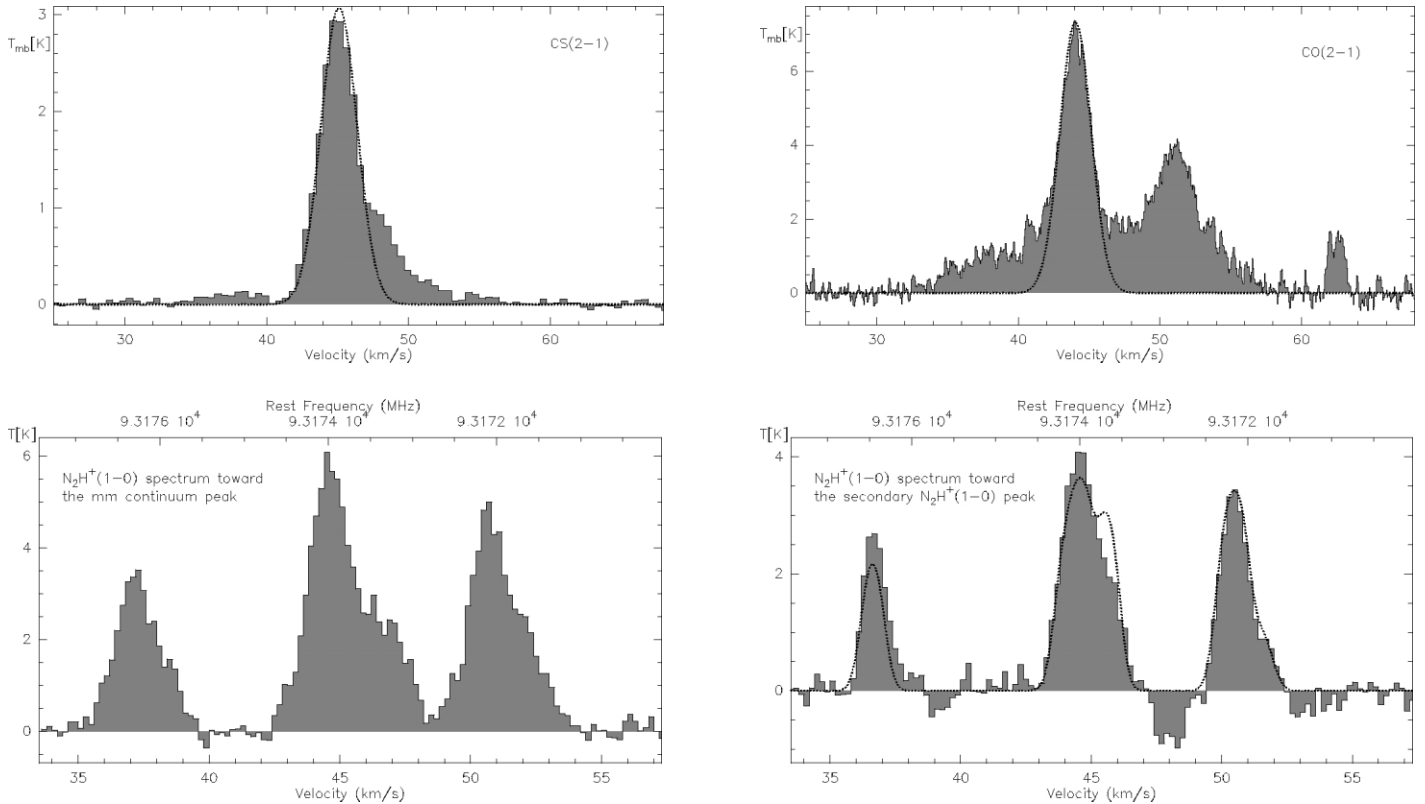


FIG. 3.—*Top*: Single-dish CS (2–1) and CO (2–1) spectra toward IRDC 18223–3 (*solid line and gray scale*), observed with the IRAM 30 m and CSO, respectively. The solid lines show the spectra, and the dotted lines give Gaussian fits to the central line component at $v_{\text{lsr}} \sim 45 \text{ km s}^{-1}$. Obviously, both spectra show strong excess line wing emission indicative of a high-velocity molecular outflow. *Bottom*: N_2H^+ (1–0) spectra in IRDC 18223–3 toward the 93 GHz continuum peak (*left*), and the secondary N_2H^+ (1–0) peak $\sim 7''$ to the east (*right*), observed with the PdBI. Note that the velocity range presented is smaller than for the CO/CS spectra. The N_2H^+ spectra cover all seven hyperfine components; the rest frequency is set to the hyperfine group frequency of 93173.770 MHz. The dotted line in the bottom right spectrum shows the fit to the hyperfine structure. The negative features in the bottom right spectrum are not real absorption features, but are due to the negative side lobes caused by the missing short spacing data in the corresponding velocity channels toward this position.

presented in Figure 3 show line-wing emission in excess of a Gaussian line component at $v_{\text{lsr}} \sim 45 \text{ km s}^{-1}$. The full width at zero intensity of both lines is $\sim 24 \text{ km s}^{-1}$. The CO (2–1) spectrum shows two additional line components at ~ 51 and $\sim 62 \text{ km s}^{-1}$. Comparing these features with CO (2–1) spectra toward other positions of the large-scale dust filament (Fig. 1), the 51 km s^{-1} component is also present toward the rest of the filament, whereas the 62 km s^{-1} component is observed only toward IRDC 18223–3. This difference indicates that the 52 km s^{-1} component is probably part of a larger scale foreground or background cloud, whereas the 62 km s^{-1} component is likely due to the molecular outflow. Following Beuther et al. (2002b), we roughly estimate the mass of high-velocity gas within the CSO primary beam ($31''$) to be $\sim 3.4 M_{\odot}$. Compared to other typical high-mass outflows (e.g., Beuther et al. 2002b), this is a relatively low value. However, since we are presumably dealing with a source at the onset of massive star formation, there has not been much time yet to eject and entrain molecular gas, and thus comparably low outflow masses are expected at this evolutionary stage.

In addition, we observed the N_2H^+ (1–0) line with seven hyperfine components around 93.174 GHz (Fig. 3), which is known to be strong and optically thin in low-mass starless cores (Tafalla et al. 2004). Figure 4 presents the N_2H^+ (1–0) emission integrated over all hyperfine components, and over a smaller velocity interval centered on the isolated N_2H^+ (1–0) component at 93,176.27 MHz. Both N_2H^+ maps show an emission peak toward the main IRDC 18223–3 millimeter continuum peak. Moreover, the N_2H^+ data exhibit a secondary peak $\sim 7''$

to the east of this main peak that is spatially associated with the MIR absorption northeast of the $4.5 \mu\text{m}$ emission. Furthermore, we find that the N_2H^+ line width Δv increases from the outer edges of the N_2H^+ emission in the direction toward the main IRDC 18223–3 millimeter peak (Fig. 4). Although the main IRDC 18223–3 peak likely exhibits multiple velocity components (see below), the general trend of increasing Δv appears real. This is indicative of increased internal motion within the main IRDC 18223–3 core—either turbulent or ordered motion, such as infall, rotation, or outflow. We interpret this as additional evidence for the onset of star formation activity. The line width is still narrow toward the IRDC 18223–3 secondary N_2H^+ peak, with $\Delta v \sim 1 \text{ km s}^{-1}$, indicating less internal motion and hence likely an earlier evolutionary stage.

Fitting the N_2H^+ hyperfine structure permits the determination of the optical depth and N_2H^+ column density (e.g., Caselli et al. 2002b). Unfortunately, we cannot derive a good fit toward the main IRDC 18223–3 millimeter peak, because the N_2H^+ spectrum shows excess emission $1\text{--}2 \text{ km s}^{-1}$ offset from the peak velocity (Fig. 3), indicative of multiple velocity components. The spectral fitting difficulties are likely due to this complex velocity structure. In contrast, we can fit the spectrum toward the secondary IRDC 18223–3 N_2H^+ peak reasonably well (Fig. 3). The resulting N_2H^+ column density of $3.1 \times 10^{13} \text{ cm}^{-2}$ translates into an H_2 column density of $N_{\text{H}_2} \sim 1.0 \times 10^{23} \text{ cm}^{-2}$, assuming a $\text{N}_2\text{H}^+/\text{H}_2$ ratio of 3×10^{-10} (Caselli et al. 2002a). Since the 3 mm continuum 3σ rms of 1.08 mJy corresponds to an H_2 column density sensitivity between 2.2×10^{23} and $5.2 \times 10^{23} \text{ cm}^{-2}$ (assuming 33

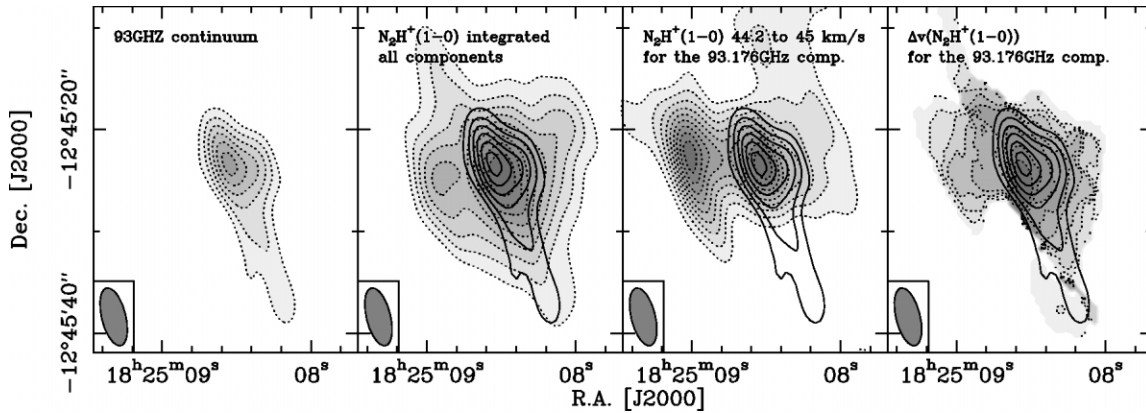


FIG. 4.—93 GHz continuum and N_2H^+ (1–0) emission and line-width maps toward IRDC 18223–3. The gray scale with thin dotted contours shows the 93 GHz continuum and N_2H^+ (1–0) maps as labeled within each panel. The solid contours in the second to fourth panels (from left to right) again show the 93 GHz continuum emission. The contouring of the continuum starts at 1.08 mJy (3σ) and proceeds in 0.72 mJy steps (2σ). The contour levels of the N_2H^+ (1–0) maps always range from 10% to 90% of the peak values ($23.5 \text{ Jy beam}^{-1}$, 1.2 Jy beam^{-1} , and 2.0 km s^{-1} , respectively). The synthesized beam is shown at the bottom left of each panel.

and 15 K, respectively), the continuum nondetection of this N_2H^+ secondary peak is a plausible observational result. Assuming a lower temperature of 15 K (typical for HMSC candidates; Sridharan et al. 2005), the 3σ mm continuum sensitivity implies that a core as massive as $37 M_\odot$ can be hidden toward this secondary N_2H^+ peak without being detected in our millimeter continuum data.

We estimate the virial masses of the IRDC 18223–3 main and secondary N_2H^+ peaks for the observed line widths Δv (2.0 and 1.0 km s^{-1} ; Fig. 4) and sizes R ($\sim 14,000 \text{ AU}$ for both peaks), following MacLaren et al. (1988). Assuming different density distributions ($\rho \propto 1/r$ and $\rho \propto 1/r^2$), the derived virial masses are $51/34$ and $13/8 M_\odot$ for the two N_2H^+ peaks, respectively. This estimate for the main N_2H^+ peak is more than a factor of 3 lower than what we derived from the 93 GHz millimeter continuum emission. Although the error budget is high for the various mass estimates (about a factor of 5; Beuther et al. 2002a), the smaller virial mass compared to the gas mass derived from the millimeter continuum is consistent with this core collapsing to form a star. The virial mass of the secondary N_2H^+ peak is consistent with the previously derived upper mass limits from the millimeter continuum. Hence, the secondary core may still be in a virially bound state, potentially prior to active star formation.

In summary, the observational features of (1) a massive IRDC, (2) a molecular outflow as suggested by the $4.5 \mu\text{m}$, CO, and CS emission, (3) the N_2H^+ line width and virial analysis, and (4) the high NH_3 temperatures indicate the presence of an extremely young massive protostellar object at the center of the millimeter continuum core IRDC 18223–3, which remains otherwise undetected in the MIR, due to its extreme youth and the high gas column densities. Although this line of evidence is still circumstantial and has to be further investigated, the MIR nondetection and the comparably low outflow mass supports an early evolutionary stage prior to the typically studied HMPOs. The narrow line width and associated virial mass of the lower mass secondary N_2H^+ peak suggests that it may be in an even younger preprotostellar stage prior to any active star formation.

IRAM is supported by INSU/CNRS (France), MPG (Germany), and IGN (Spain). *Spitzer* is operated by the JPL, Caltech under NASA contract 1407. We wish to thank J. Hora, C. de Vries, J. Joergensen, T. Bourke, T. Megeath, and T. Huard for help with the *Spitzer* and N_2H^+ data. We also thank the referee for detailed comments improving the paper. H. B. acknowledges financial support by the Emmy-Noether-Programm of the Deutsche Forschungsgemeinschaft (grant BE2578).

REFERENCES

- Alves, J. F., Lada, C. J., & Lada, E. A. 2001, *Nature*, 409, 159
 Andre, P., Ward-Thompson, D., & Barsony, M. 2000, in *Protostars and Planets IV*, ed. V. Mannings, A. P. Boss, & S. S. Russell (Tucson: Univ. Arizona Press), 59
 Bacmann, A., André, P., Puget, J.-L., Abergel, A., Bontemps, S., & Ward-Thompson, D. 2000, *A&A*, 361, 555
 Benjamin, R. A., et al. 2003, *PASP*, 115, 953
 Beuther, H., Schilke, P., & Stanke, T. 2003, *A&A*, 408, 601
 Beuther, H., et al. 2002a, *ApJ*, 566, 945
 ———. 2002b, *A&A*, 383, 892
 Caselli, P., Benson, P. J., Myers, P. C., & Tafalla, M. 2002a, *ApJ*, 572, 238
 Caselli, P., et al. 2002b, *ApJ*, 565, 344
 Churchwell, E. 2002, *ARA&A*, 40, 27
 Egan, M. P., et al. 1998, *ApJ*, 494, L199
 Fazio, G. G., et al. 2004, *ApJS*, 154, 10
 Frerking, M. A., Langer, W. D., & Wilson, R. W. 1982, *ApJ*, 262, 590
 Garay, G., et al. 2004, *ApJ*, 610, 313
 Hill, T., et al. 2005, *MNRAS*, 363, 405
 Kirk, J. M., Ward-Thompson, D., & André, P. 2005, *MNRAS*, 360, 1506
 Klein, R., Posselt, B., Schreyer, K., Forbrich, J., & Henning, T. 2005, *ApJS*, 161, in press
 Kurtz, S., Cesaroni, R., Churchwell, E., Hofner, P., & Walmsley, C. M. 2000, in *Protostars and Planets IV*, ed. V. Mannings, A. P. Boss, & S. S. Russell (Tucson: Univ. Arizona Press), 299
 MacLaren, I., Richardson, K. M., & Wolfendale, A. W. 1988, *ApJ*, 333, 821
 Molinari, S., Brand, J., Cesaroni, R., & Palla, F. 1996, *A&A*, 308, 573
 Noriega-Crespo, A., et al. 2004, *ApJS*, 154, 352
 Richer, J. S., Shepherd, D. S., Cabrit, S., Bachiller, R., & Churchwell, E. 2000, in *Protostars and Planets IV*, ed. V. Mannings, A. P. Boss, & S. S. Russell (Tucson: Univ. Arizona Press), 867
 Sridharan, T. K., Beuther, H., Saito, M., Wyrowski, F., & Schilke, P. 2005, *ApJ*, 634, in press
 Sridharan, T. K., Beuther, H., Schilke, P., Menten, K. M., & Wyrowski, F. 2002, *ApJ*, 566, 931
 Tafalla, M., Myers, P. C., Caselli, P., & Walmsley, C. M. 2004, *A&A*, 416, 191
 Werner, M. W., et al. 2004, *ApJS*, 154, 1